Volume 12
Number 2
14 January 2021
Pages 495–816

Chemical Science

rsc.li/chemical-science

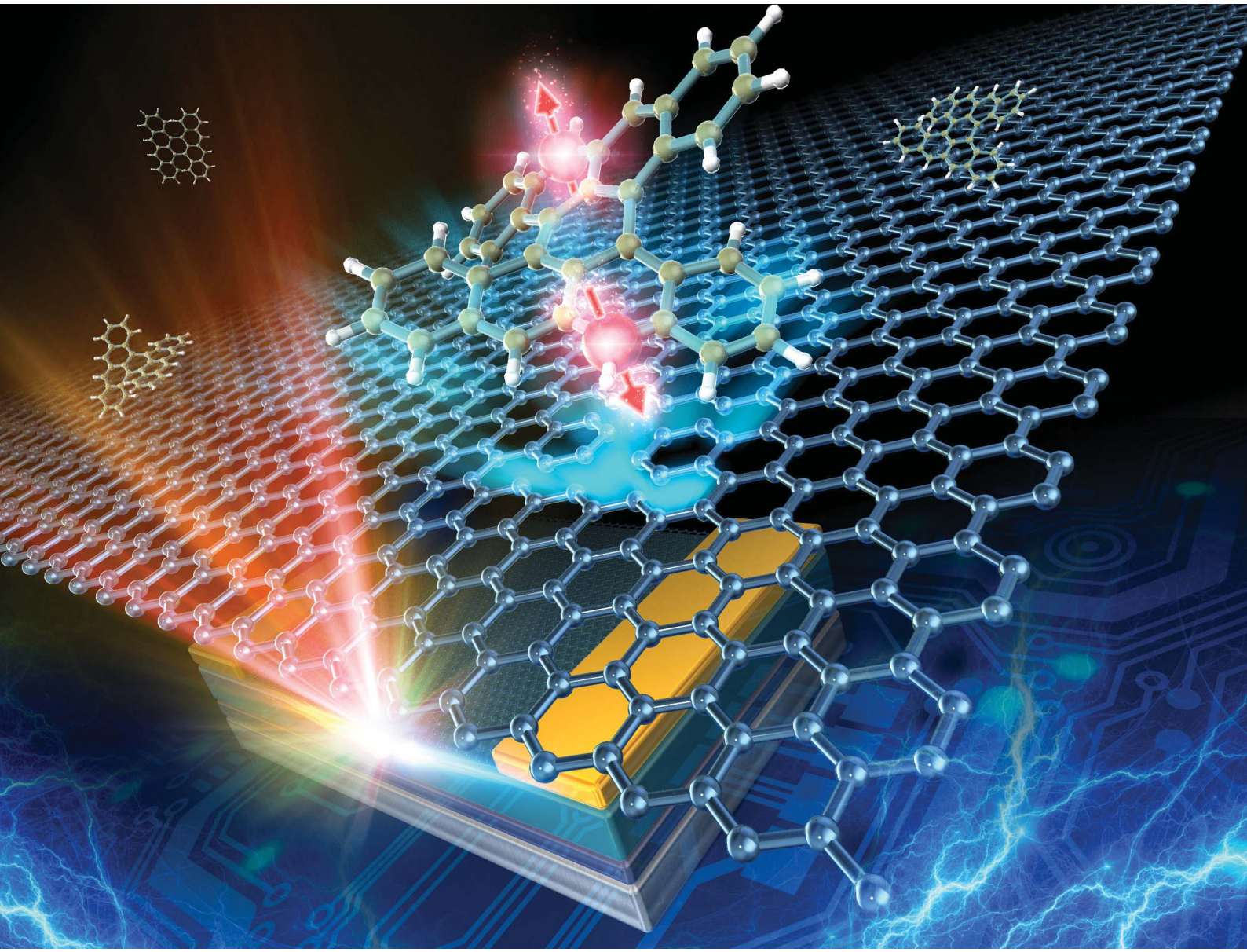

ISSN 2041-6539

ROYAL SOCIETY OF CHEMISTRY

EDGE ARTICLE

Masashi Mamada, Chihaya Adachi *et al.*
Synthesis, crystal structure and charge transport characteristics of stable *peri*-tetracene analogues

Chemical Science

ROYAL SOCIETY OF CHEMISTRY

EDGE ARTICLE

View Article Online
View Journal | View Issue

Cite this: *Chem. Sci.*, 2021, **12**, 552

All publication charges for this article have been paid for by the Royal Society of Chemistry

Received 26th August 2020
Accepted 13th October 2020

DOI: 10.1039/d0sc04699j

rsc.li/chemical-science

Synthesis, crystal structure and charge transport characteristics of stable *peri*-tetracene analogues†

Masashi Mamada, *[abc] Ryota Nakamura[ab] and Chihaya Adachi *[abcd]

peri-Acenes have shown great potential for use as functional materials because of their open-shell singlet biradical character. However, only a limited number of *peri*-acene derivatives larger than *peri*-tetracene have been synthesized to date, presumably owing to the low stability of the target compounds in addition to the complicated synthesis scheme. Here, a very simple synthesis route for the tetrabenzo[*a*,*f*,*j*,*o*]perylene (TBP) structure enables the development of highly stable *peri*-tetracene analogues. Despite a high degree of singlet biradical character, the compounds with four substituents at the zigzag edge show a remarkable stability in solution under ambient conditions, which is better than that of acene derivatives with a closed-shell electronic configuration. The crystal structures of the TBP derivatives were obtained for the first time; these are valuable to understand the relationship between the structure and biradical character of *peri*-acenes. The application of *peri*-acenes in electronic devices should also be investigated. Therefore, the semiconducting properties of the TBP derivative were investigated by fabricating the field-effect transistors.

Introduction

Acenes and functionalized acenes, which are a class of polycyclic aromatic hydrocarbons (PAHs) with laterally fused benzene rings, have received considerable attention because of their attractive properties that include high mobility and efficient multi-excitonic processes like singlet fission and triplet–triplet upconversion.[1–3] Thus, they have been applied to various organic electronic devices such as organic field-effect transistors (OFETs)[4] and organic light-emitting diodes (OLEDs).[5] Larger acenes having more than six benzene rings are known to have an open-shell (OS) singlet biradical character and are also promising for use in optoelectronic devices. However, their intrinsically low stability has hindered a detailed study of these materials.[6]

Additionally, interest in *peri*-fused systems, so-called *peri*-acenes and acenoacenes, has been increasing because such zigzag-edged PAHs are considered to be nanographenes.[7] Examples of *peri*-acenes are shown in Fig. 1, where the compounds have a conjugated system with two rows of acenes. Although perylene[8] and bisanthene,[9] as the smaller π-systems, have been known for a long time, teranthene,[10] tetrabenzo[*a*,*f*,*j*,*o*]perylene (TBP)[11] and *peri*-tetracene[12,13] were synthesized only very recently, and *peri*-pentacenes have only

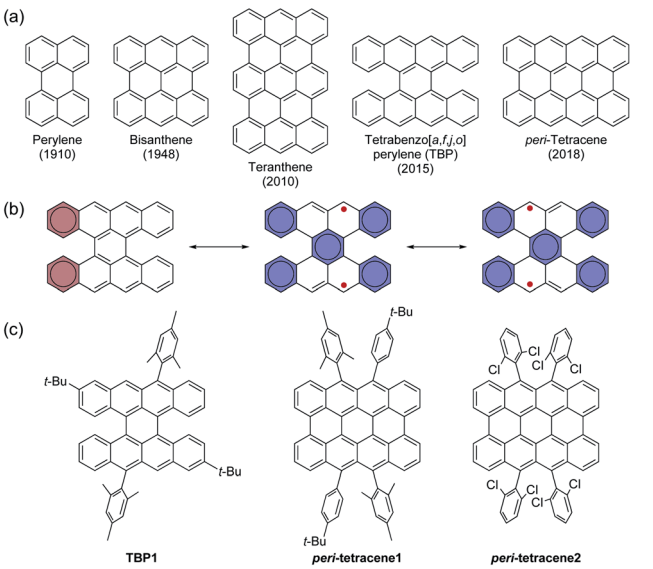

Fig. 1 (a) Chemical structures of *peri*-acenes. (b) Resonance structures of TBP and *peri*-tetracene. (c) Structures of the reported TBP and *peri*-tetracene derivatives.

[a]*Center for Organic Photonics and Electronics Research (OPERA), Kyushu University, Fukuoka 819-0395, Japan. E-mail: mamada@opera.kyushu-u.ac.jp; adachi@cstf.kyushu-u.ac.jp*

[b]*JST, ERATO, Adachi Molecular Exciton Engineering Project c/o Center for Organic Photonics and Electronics Research (OPERA), Kyushu University, Nishi, Fukuoka 819-0395, Japan*

[c]*Academia-Industry Molecular Systems for Devices Research and Education Center (AIMS), Kyushu University, Nishi, Fukuoka 819-0395, Japan*

[d]*International Institute for Carbon Neutral Energy Research (WPI-I2CNER), Kyushu University, Nishi, Fukuoka 819-0395, Japan*

† Electronic supplementary information (ESI) available: Synthesis, characterization, computational, photophysical, electrochemical and thin-film transistor data. CCDC 2025243 and 2025244. For ESI and crystallographic data in CIF or other electronic format see DOI: 10.1039/d0sc04699j

been obtained in ultrahigh vacuum conditions.[14] These larger π-systems can exhibit a significant singlet biradical feature and unique properties. The OS singlet biradical contributions in their resonance structures result from the additional Clar's aromatic sextets in the biradical form. Fig. 1b shows the resonance structures of TBP, where the closed-shell (CS) form has two aromatic sextets while the OS form has five aromatic sextets, which indicates a large biradical character for TBP. Note that the radicals in the allylic positions can be delocalized and stabilized, which results in a large spin density at the four carbon atoms found at the zigzag edges. The resonance structures of *peri*-tetracene are essentially similar to that of TBP, therefore referred to as *peri*-tetracene analogue for TBP in this paper, although the biradical character of *peri*-tetracene is higher than that of TBP because of the larger conjugation in the planar structure of *peri*-tetracene. To date, there have been few examples of the precisely synthesized and isolated derivatives of TBP and *peri*-tetracene (Fig. 1c).[11,12] Because singlet biradical materials are generally unstable, these three molecules also decompose quickly in solution. Therefore, the stability needs to be improved for their further applications in electronic devices. However, their complicated synthesis schemes hinder the preparation of derivatives with various substituents. Consequently, the properties of *peri*-tetracene analogues are not fully understood.

In this study, we developed a simple synthetic route for various TBP derivatives, which can potentially be used for the synthesis of *peri*-tetracenes. The synthesis scheme allows us to obtain TBP derivatives with two or four substituents at the 9,20- or 9,10,19,20-positions, respectively, which results in a significant improvement of the stability. In addition, OFET devices comprising the TBP derivatives have been investigated and show a good bipolar charge transport property despite the non-planar structure of the TBP core.

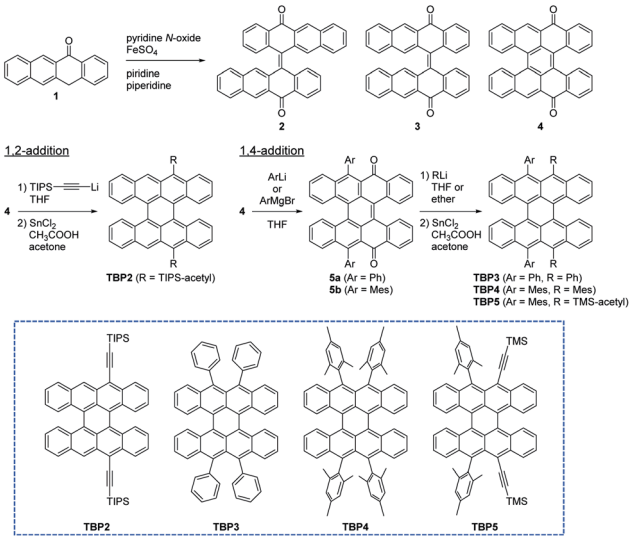

Scheme 1 Chemical structures of new TBP derivatives (TBP2–5) and synthesis routes.

Results and discussion

Synthesis

The synthesis procedures for the new TBP derivatives (**TBP2–TBP5**) are shown in Scheme 1 and Method S1 (see the ESI†). The key intermediate in our strategy was compound **4** (tetrabenzo [*a*,*f*,*j*,*o*]perylene-9,20-dione) based on the fact that many acene derivatives can be synthesized from acene quinones.[15] This also enabled the introduction of various substituents/protecting groups in the last step, in contrast to the synthesis methods for the previously reported **TBP1** and *peri*-tetracenes, which require the introduction of substituents in the early steps. We found that **4** was formed as a trace byproduct under the reaction conditions (at 100 °C for 5 h) for the synthesis of **2** and **3**,[16] and **4** could be obtained as the main product by optimizing the reaction temperature and time (at 120 °C for 48 h). Compound **4** was also obtained from an isolated mixture of **2** and **3** (inseparable *E* and *Z* isomers), which suggested a sequential two-step reaction from **1**. According to Clar's rule,[17] **4** is considered to have a large contribution of the resonance structure with five aromatic sextets, which results in a clear α,β-unsaturated carbonyl structure (see Crystal structure section below). For the reaction between **4** and organolithium reagents, both 1,2-addition (a direct nucleophilic attack at the carbonyl group) and 1,4-addition (Michael addition) were observed depending on the nucleophiles involved. Similar to the synthesis of TIPS-pentacene from pentacenequinone,[18] TIPS-acetylene-substituted TBP (**TBP2**) was synthesized by the nucleophilic 1,2-addition of lithium acetylide, followed by reduction using $SnCl_2$ in low yield (<1%), where the products of the 1,4-addition were obtained in trace amounts. Although lithium and Grignard reagents tend to promote a 1,2-addition, aryl lithium and aryl Grignard reagents with **4** lead to Michael addition rather than 1,2-addition to give compounds **5a** and **5b** as the main products with a small amount of by-products from a 1,2-addition, probably owing to the steric congestion from the rigid core structure.[19] Therefore, four-substituted TBP (**TBP3–TBP5**) could be synthesized through a second nucleophilic addition.[18] Therefore, we successfully obtained new TBP derivatives in a few short steps. Although we focused on TBP derivatives in this work, **4** will undergo intramolecular coupling by a Scholl reaction to give a fully planar fused compound (see the ESI†), which can be used as a precursor of *peri*-tetracene.

Optical and electrochemical properties and stability test

Because all of the new compounds (**TBP2–TBP5**) are based on the TBP core, their properties, which include the biradical character, should be similar to those of **TBP1**, which has already been determined to have an OS singlet biradical nature by UV-vis absorption spectroscopy, theoretical calculations, electron spin resonance (ESR) spectroscopy and variable-temperature (VT) NMR spectroscopy.[11] To realize stable singlet biradical compounds, it is important to protect the position with a high spin density (9,10,19,20-positions of the TBP core). **TBP2** has a thermodynamic stabilization that extends the conjugation and delocalizes radicals by the

introduction of substituents, such as acetylene, although only two positions are protected. On the other hand, **TBP1**, **TBP3** and **TBP4** are kinetically stabilized by bulky protecting groups. A mesityl group is bulkier than a phenyl group, which indicates a better protection for the singlet biradical of **TBP4**. **TBP5** is expected to be stabilized by both a thermodynamic and kinetic approach.

Fig. 2 shows UV-vis absorption spectra in dichloromethane (DCM). The solutions of **TBP2–TBP5** were green because of the absorption band in the range of the red to near-infrared (NIR) region. The results clearly showed a red shift of the lowest energy band in the NIR region for the compounds with acetyl groups. The absorption maxima (λ_{max}) were 765, 733, 729 and 783 nm for **TBP2–TBP5**, respectively, which indicated a narrow HOMO–LUMO gap and high biradical character for these compounds that were similar to those for **TBP1** with an absorption maximum at 727 nm. In fact, the theoretical calculations of the biradical character (y_0) using Yamaguchi's scheme at the UHF/6-31G(d,p) level were 0.60, 0.62, 0.60, 0.59 and 0.62 for **TBP1–TBP5**, respectively (full data of the calculations can be found in the ESI, Methods S2, Tables S1–S4, and Fig. S1–S4†).[20] However, these singlet biradical features generally led to a fast decomposition of the compounds by photooxidation in air. In fact, the absorption spectra of most of the acenes quickly changed, which indicated a low stability. The changes of the absorption intensity at λ_{max} under white room light in ambient air are summarized in Fig. 2b and each spectrum is shown in Fig. 2c–f. These results demonstrated the significant difference in stability of these compounds. The decompositions of **TBP2** and **TBP3** took place on a similar time scale, which was faster than that of rubrene,[21] because of the higher singlet biradical character of the *peri*-acenes. Thus, the absorption intensity almost disappeared after several hours, as shown in Fig. 2c and d. The colour of the solution changed to yellow, then red-purple, likely owing to the addition of oxygen and the formation of carbonyl groups (Fig. S5 in the ESI†). Because **TBP2** had only two substituents and **TBP3** had less sterically crowded phenyl rings, the protection of the radicals was expected to be limited. Although the experimental conditions were not exactly the same as those in previous reports by keeping the samples under ambient light, the photostability of **TBP1**, which showed a *ca.* 50% absorption intensity after 20 min, is likely to be similar to that of **TBP2** and **TBP3**. On the other hand, **TBP4** with four bulky mesityl groups showed a much better stability than rubrene with only a slight degradation in ambient conditions. In addition, the spectra of **TBP5** exhibited no significant changes of the intensity even after a week. These results indicated that the trialkylsilylacetylene groups have a better protection property than the mesityl groups. Therefore, a highly stable molecule with an OS singlet ground state could be obtained. This improvement enables an easy handling of the solution for fabricating organic electronic devices that require high purity.

The emission spectra of **TBP4** and **TBP5** are shown in Fig. S6 in the ESI.† The compounds showed NIR emission with emission maxima of 888 nm and 934 nm and a small full width at half maximum (FWHM) of 127 nm (0.19 eV) and 80 nm (0.11 eV) for **TBP4** and **TBP5**, respectively. However, the quantum yields were very low (<0.5%) for both compounds.

The results of the cyclic voltammetry (CV) for **TBP4** and **TBP5** showed two reversible oxidation and reduction peaks (Fig. S7 and Table S5 in the ESI†). The first oxidation and reduction

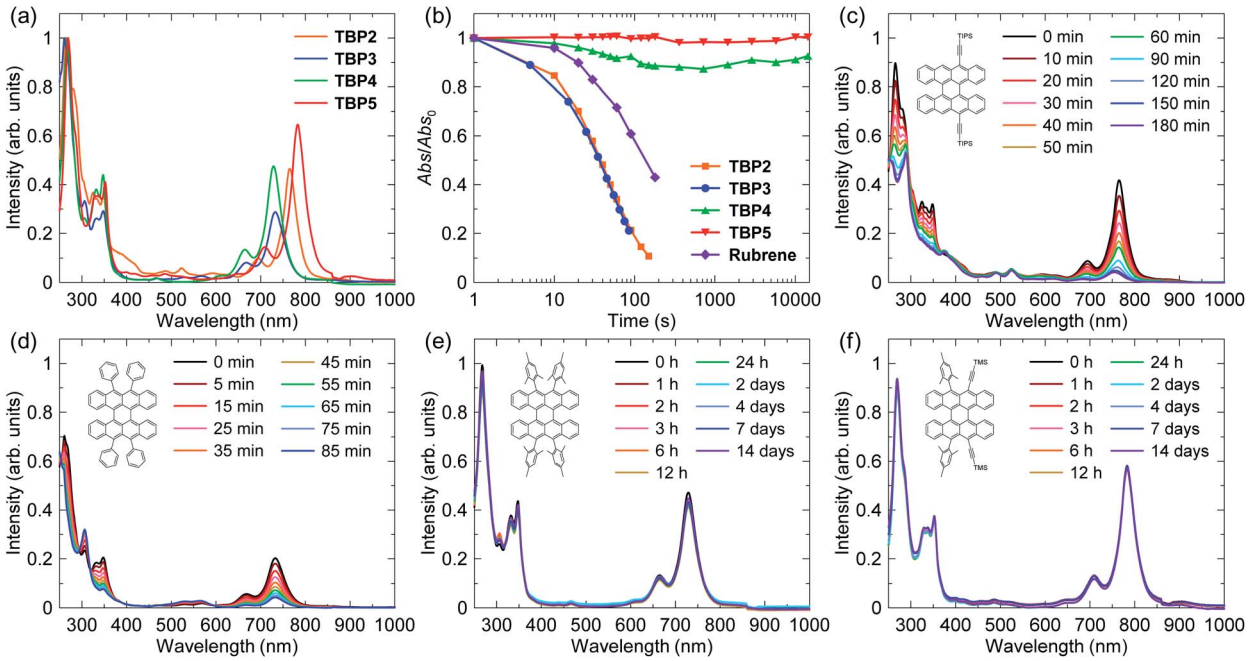

Fig. 2 UV-vis absorption spectra for (a) **TBP2–TBP5** in DCM. (b) Absorbance normalized to the initial absorbance for **TBP2–TBP5** at their λ_{max} (765, 733, 729, 783 and 527 nm, respectively) and rubrene as a function of time under ambient white light in air saturation. UV-vis absorption spectra as a function of time for (c) **TBP2**, (d) **TBP3**, (e) **TBP4** and (f) **TBP5**.

peaks *vs.* ferrocene/ferrocenium were at −0.07 V and −1.64 V for **TBP4** and 0 V and −1.37 V for **TBP5**, respectively. The energy gaps of 1.57 eV and 1.37 eV agreed well with optical gaps of these compounds.

Single crystal structure

The single crystals of compounds **5b**, **TBP4** and **TBP5** were obtained by the slow recrystallization from DCM layered with MeOH (Fig. 3, Methods S3, Tables S6 and S7, Fig. S8 and S9 in the ESI†). The crystals of **5b** and **TBP5** included DCM solvent molecules. Unfortunately, the quality of data for **TBP4** were not sufficiently high ($R > 20\%$) because of the very weak reflections. Therefore, the data are provided in the ESI† without the detailed discussions of the bond lengths. However, we were able to confirm the structure and packing motif.

All the compounds showed an intersecting conformation of two tetracene subunits (Fig. S1†), where the central ring E was twisted (Fig. 3f). The bond lengths of compound **5b** indicated the contribution of α,β-unsaturated carbonyl structures, where α,β-unsaturated C=C bond (bond *p*) is short compared with a tetracene quinone derivative,[22] as observed in a *peri*-pentacene derivative that undergoes Michael addition.[19] In addition, the slightly increased bond lengths for bonds *i*, *m* and *o* suggested a decrease of the aromaticity in ring B. These features enabled a Michael addition reaction to compound **4**. Although the crystal structure of ***peri*-tetracene2** shown in Fig. 1 has been investigated,[12b] there has been no report for the crystal structure of the TBP derivatives. Therefore, the crystal data of **TBP5** would be important to confirm the biradical characters of TBP derivatives. Although the torsion angle for the two tetracene units were relatively large for **TBP5** (*ca.* 40°), the bond lengths for bonds *v* and *w* were still short (1.448 Å) and only slightly longer than that of ***peri*-tetracene2** (1.442 Å), which indicated a biradical contribution owing to electronic coupling between two tetracene units. The degree of bond alternation was similar to that of ***peri*-tetracene2**. These results strongly support the high biradical character of TBP derivatives. Note that the calculated bond lengths well agreed with the experimental result (Fig. S8†).

The packing structure, which may give some insight to the charge transport property, is shown in Fig. 3c for **TBP5**. The packing structure of **TBP4** is shown in Fig. S9,† where the interactions between TBP cores seemed to be very small. For **TBP5**, a herringbone packing with a tilt angle of 42° was observed in the horizontal direction. The distance of the CH–π interaction was 2.785 Å, which is comparable to that for pentacene in the *peri*-direction. Although the intermolecular interactions are limited because of the relatively large substitution groups, the results proved that efficient charge transport in **TBP5** is possible.

VT NMR and ESR

The ^{1}H NMR spectra of **TBP4** in DCM-d_2 showed broad peaks at room temperature (Fig. 4a), which is often observed for OS singlet biradicals because triplet biradicals are thermally accessible. Therefore, the peaks became sharper by decreasing the temperature and were assigned to the structure of **TBP4** with the help of 2D-COSY NMR spectroscopy. The broad peaks at room temperature were found to be from H3 (7.08 ppm, double doublet at 193 K) and H1 (7.26 ppm, doublet at 193 K). This result agrees well with the relatively high spin density distribution at these positions calculated by density functional theory (DFT) at the UB3LYP/6-311G(d,p) level. The singlet biradical feature was further characterized by an ESR measurement in the solid state, which gave a typical ESR signal with a *g*-value of

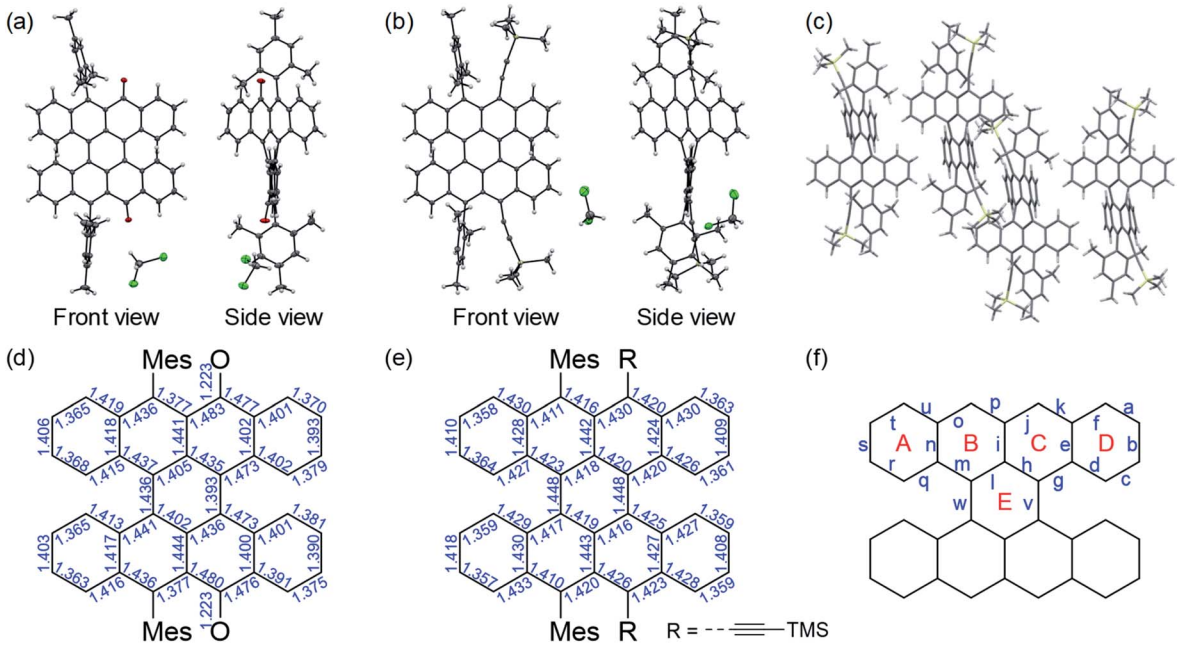

Fig. 3 X-ray crystal structures of (a) **5b** and (b) **TBP5**. (c) Packing structure of **TBP5**. Bond lengths in the crystals of (d) **5b** and (e) **TBP5**. (f) Positions of bonds and rings.

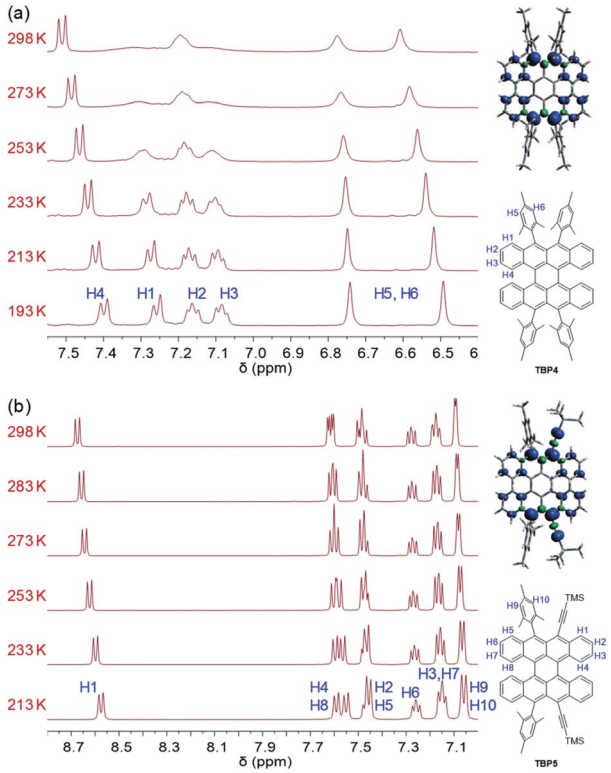

Fig. 4 VT ^{1}H-NMR spectra of (a) **TBP4** and (b) **TBP5** in DCM-d_2 in the aromatic region.

2.003 for **TBP4** (Fig. S10 in the ESI†). On the other hand, **TBP5** showed a weaker ESR signal and negligible broadening of the NMR peaks at room temperature, which indicated a larger singlet–triplet energy gap (ΔE_{S-T}) (Fig. 4b). The theoretical calculations showed a smaller ΔE_{S-T}, calculated by geometry optimization for the singlet and triplet states, for **TBP5** than **TBP4**, which was not consistent with the NMR results. However, the time-dependent (TD)-DFT calculations showed a larger vertical excitation energy of **TBP5** than **TBP4** for the triplet in the singlet ground state geometry, suggesting that the different activation energies for the triplet caused the different degrees of broadening. Because some recent papers have reported a high biradical character with a large ΔE_{S-T},[23,24] this should be investigated in more detail in future works.

Charge transport properties

The OFET devices using **TBP5** were investigated because of its higher stability and better interactions. The devices with bottom-gate/top-contact (BG/TC) configurations were fabricated for the drop-coated films from an *o*-dichlorobenzene (ODCB) solution on a cross-linked poly-4-vinylphenol (PVP) dielectric layer (see Methods S4 and Fig. S11 in the ESI†). Some recent reports used several types of singlet biradical compounds for the active layer of OFETs, which revealed their bipolar transport owing to small energy gaps.[24–26] The **TBP**-based devices also demonstrated a capability of bipolar transport for *peri*-acene derivatives. Fig. 5 shows the transfer and output characteristics with hole and electron mobilities of 1.6×10^{-3} and 6.1×10^{-5}

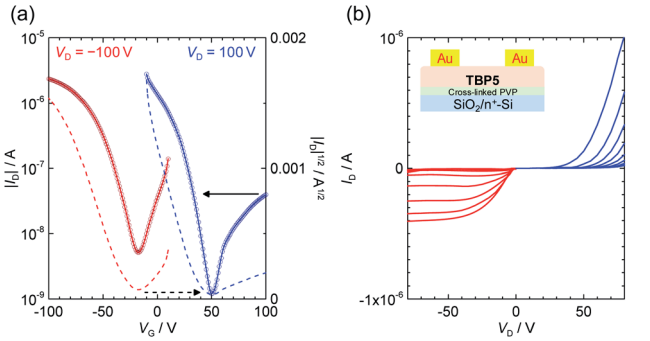

Fig. 5 OFET devices of **TBP5**. (a) Transfer and (b) output characteristics of a BG/TC device with a drop-casted film from 0.3 wt% ODCB solution.

cm^2 V^{-1} s^{-1}, respectively. The devices obtained from the different drop-casting conditions, which have different degree of crystalline domains, showed a higher hole mobility of 1.2×10^{-2} cm^2 V^{-1} s^{-1}, although the electron transport was not clear because of a largely unbalanced hole and electron currents (Fig. S12 in the ESI†). The crystallinity of the thin-films was evaluated by X-ray diffraction (XRD), polarized optical microscopy (POM) and atomic force microscopy (AFM) (see Fig. S13 and 14 in the ESI†). The out-of-plane XRD showed a small peak at $2\theta = 9.28°$ ($d = 9.5$ Å). This was shorter than the molecular length (*ca.* 11 Å for the tetracene length and 19 Å in the substitution direction). Therefore, the molecules may have had declined orientations on the substrate. The microscopy images also confirmed polycrystalline domains in the channel.

Overall, *peri*-acene derivatives show a high potential for use as organic semiconducting materials.

Conclusions

In this work, we have developed a new synthesis route for TBP derivatives of a *peri*-tetracene analogue, which is much simpler and shorter than the previously reported methods. The newly developed TBP derivatives with four substituents showed a higher stability than rubrene in solution under ambient conditions despite a higher singlet biradical character. Thus, the simple protection approach is found to be an effective method to improve the stability of *peri*-acenes. The crystal structures of TBP derivatives were obtained for the first time and clearly revealed a large biradical contribution in the TBP structure. The charge transport properties of the TBP derivative were also investigated for the first time and the results clearly demonstrated a bipolar nature for the *peri*-tetracenes.

Conflicts of interest

There are no conflicts to declare.

Acknowledgements

We thank Ms K. Kusuhara and Ms N. Nakamura for the materials characterization, Mr T. Matsumoto for the measurements

of X-ray single crystal analysis. This work was financially supported by JST ERATO Grant Number JPMJER1305, JSPS KAKENHI Grant Number 19H02790, and the JSPS Core-to-Core Program.

Notes and references

1 (*a*) Q. Ye and C. Chi, *Chem. Mater.*, 2014, **26**, 4046–4056; (*b*) Z. Sun, Q. Ye, C. Chi and J. Wu, *Chem. Soc. Rev.*, 2012, **41**, 7857–7889.

2 (*a*) W. Warta and N. Karl, *Phys. Rev. B: Condens. Matter Mater. Phys.*, 1985, **32**, 1172–1182; (*b*) J. E. Anthony, *Chem. Rev.*, 2006, **106**, 5028–5048; (*c*) C. Wang, H. Dong, W. Hu, Y. Liu and D. Zhu, *Chem. Rev.*, 2012, **112**, 2208–2267.

3 (*a*) M. B. Smith and J. Michl, *Chem. Rev.*, 2010, **110**, 6891–6936; (*b*) D. N. Congreve, J. Lee, N. J. Thompson, E. Hontz, S. R. Yost, P. D. Reusswig, M. E. Bahlke, S. Reineke, T. Van Voorhis and M. A. Baldo, *Science*, 2013, **340**, 334–337; (*c*) E. G. Fuemmeler, S. N. Sanders, A. B. Pun, E. Kumarasamy, T. Zeng, K. Miyata, M. L. Steigerwald, X.-Y. Zhu, M. Y. Sfeir, L. M. Campos and N. Ananth, *ACS Cent. Sci.*, 2016, **2**, 316–324; (*d*) R. G. Kepler, J. C. Caris, P. Avakian and E. Abramson, *Phys. Rev. Lett.*, 1963, **10**, 400–402.

4 (*a*) A. N. Aleshin, J. Y. Lee, S. W. Chu, J. S. Kim and Y. W. Park, *Appl. Phys. Lett.*, 2004, **84**, 5383–5385; (*b*) T. W. Kelley, D. V. Muyres, P. F. Baude, T. P. Smith and T. D. Jones, *Mater. Res. Soc. Symp. Proc.*, 2003, **771**, 169–179; (*c*) K. Ito, T. Suzuki, Y. Sakamoto, D. Kubota, Y. Inoue, F. Sato and S. Tokito, *Angew. Chem., Int. Ed.*, 2003, **42**, 1159–1162; (*d*) A. Afzali, C. D. Dimitrakopoulos and T. L. Breen, *J. Am. Chem. Soc.*, 2002, **124**, 8812–8813.

5 (*a*) D. Y. Kondakov, T. D. Pawlik, T. K. Hatwar and J. P. Spindler, *J. Appl. Phys.*, 2009, **106**, 124510; (*b*) B. H. Wallikewitz, D. Kabra, S. Gélinas and R. H. Friend, *Phys. Rev. B: Condens. Matter Mater. Phys.*, 2010, **85**, 045209; (*c*) R. Ieuji, K. Goushi and C. Adachi, *Nat. Commun.*, 2019, **10**, 5283; (*d*) R. Nagata, H. Nakanotani, W. J. Potscavage Jr and C. Adachi, *Adv. Mater.*, 2018, **30**, 1801484.

6 (*a*) M. M. Payne, S. R. Parkin and J. E. Anthony, *J. Am. Chem. Soc.*, 2005, **127**, 8028–8029; (*b*) R. Mondal, R. M. Adhikari, B. K. Shah and D. C. Neckers, *Org. Lett.*, 2007, **9**, 2505–2508; (*c*) M. Watanabe, Y. J. Chang, S.-W. Liu, T.-H. Chao, K. Goto, M. M. Islam, C.-H. Yuan, Y.-T. Tao, T. Shinmyozu and T. J. Chow, *Nat. Chem.*, 2012, **4**, 574–578; (*d*) D. Chun, Y. Cheng and F. Wudl, *Angew. Chem., Int. Ed.*, 2008, **47**, 8380–8385; (*e*) H. Qu and C. Chi, *Org. Lett.*, 2010, **12**, 3360–3363; (*f*) B. Purushothaman, S. R. Parkin and J. E. Anthony, *Org. Lett.*, 2010, **12**, 2060–2063.

7 (*a*) L. A. Stevens, K. P. Goetz, A. Fonari, Y. Shu, R. M. Williamson, J.-L. Brédas, V. Coropceanu, O. D. Jurchescu and G. E. Collis, *Chem. Mater.*, 2015, **27**, 112–118; (*b*) L. Zhang, A. Fonari, Y. Liu, A. L. Hoyt, H. Lee, D. Granger, S. Parkin, T. P. Russell, J. E. Anthony, J.-L. Brédas, V. Coropceanu and A. L. Briseno, *J. Am. Chem. Soc.*, 2014, **136**, 9248–9251; (*c*) K. Sbargoud, M. Mamada, T. Jousselin-Oba, Y. Takeda, S. Tokito, A. Yassar, J. Marrot and M. Frigoli, *Chem.–Eur. J.*, 2017, **23**, 5076–5080; (*d*) C. Reus, M. P. Lechner, M. Schulze, D. Lungerich, C. Diner, M. Gruber, J. M. Stryker, F. Hampel, N. Jux and R. R. Tykwinski, *Chem.–Eur. J.*, 2016, **22**, 9097–9101; (*e*) Z. Wang, R. Li, Y. Chen, Y. Tan, Z. Tu, X. Gao, H. Dong, Y. Yi, Y. Zhang, W. Hu, K. Müllen and L. Chen, *J. Mater. Chem. C*, 2017, **5**, 1308–1312; (*f*) X. Liu, M. Chen, C. Xiao, N. Xue and L. Zhang, *Org. Lett.*, 2018, **20**, 4512–4515; (*g*) T. Dumslaff, B. Yang, A. Maghsoumi, G. Velpula, K. S. Mali, C. Castiglioni, S. D. Feyter, M. Tommasini, A. Narita, X. Feng and K. Müllen, *J. Am. Chem. Soc.*, 2016, **138**, 4726–4729; (*h*) Q. Wang, T. Y. Gopalakrishna, H. Phan, T. S. Herng, S. Dong, J. Ding and C. Chi, *Angew. Chem., Int. Ed.*, 2017, **56**, 11415–11419; (*i*) Q. Chen, D. Wang, M. Baumgarten, D. Schollmeyer, K. Müllen and A. Narita, *Chem.–Asian J.*, 2019, **14**, 1703–1707; (*j*) X. Xu, K. Müllen and A. Narita, *Bull. Chem. Soc. Jpn.*, 2020, **93**, 490–506.

8 (*a*) R. Scholl and J. Mansfeld, *Ber. Dtsch. Chem. Ges.*, 1910, **43**, 1734–1746; (*b*) R. Scholl, C. Seer and R. Weitzenböck, *Ber. Dtsch. Chem. Ges.*, 1910, **43**, 2202–2209.

9 (*a*) E. Clar, *Chem. Ber.*, 1948, **81**, 52–63; (*b*) E. Clar, *Chem. Ber.*, 1949, **82**, 46–60; (*c*) E. H. Fort, P. M. Donovan and L. T. Scott, *J. Am. Chem. Soc.*, 2009, **131**, 16006–16007; (*d*) H. Hayashi, N. Aratani and H. Yamada, *Chem.–Eur. J.*, 2017, **12**, 7000–7008.

10 (*a*) A. Konishi, Y. Hirao, M. Nakano, A. Shimizu, E. Botek, B. Champagne, D. Shiomi, K. Sato, T. Takui, K. Matsumoto, H. Kurata and T. Kubo, *J. Am. Chem. Soc.*, 2010, **132**, 11021–11023; (*b*) A. Konishi, Y. Hirao, K. Matsumoto, H. Kurata, R. Kishi, Y. Shigeta, M. Nakano, K. Tokunaga, K. Kamada and T. Kubo, *J. Am. Chem. Soc.*, 2013, **135**, 1430–1437.

11 J. Liu, P. Ravat, M. Wagner, M. Baumgarten, X. Feng and K. Müllen, *Angew. Chem., Int. Ed.*, 2015, **54**, 12442–12446.

12 (*a*) M. R. Ajayakumar, Y. Fu, J. Ma, F. Hennersdorf, H. Komber, J. J. Weigand, A. Alfonsov, A. A. Popov, R. Berger, J. Liu, K. Müllen and X. Feng, *J. Am. Chem. Soc.*, 2018, **140**, 6240–6244; (*b*) Y. Ni, T. Y. Gopalakrishna, H. Phan, T. S. Herng, S. Wu, Y. Han, J. Ding and J. Wu, *Angew. Chem., Int. Ed.*, 2018, **57**, 9697–9701.

13 (*a*) S. Mishra, T. G. Lohr, C. A. Pignedoli, J. Liu, R. Berger, J. I. Urgel, K. Müllen, X. Feng, P. Ruffieux and R. Fasel, *ACS Nano*, 2018, **12**, 11917–11927; (*b*) M. R. Ajayakumar, Y. Fu, F. Liu, H. Komber, V. Tkachova, C. Xu, S. Zhou, A. A. Popov, J. Liu and X. Feng, *Chem.–Eur. J.*, 2020, **26**, 7497–7503; (*c*) X. Liu, M. Chen, C. Xiao, N. Xue and L. Zhang, *Org. Lett.*, 2018, **20**, 4512–4515.

14 (*a*) C. Rogers, C. Chen, Z. Pedramrazi, A. A. Omrani, H.-Z. Tsai, H. S. Jung, S. Lin, M. F. Crommie and F. R. Fischer, *Angew. Chem., Int. Ed.*, 2015, **54**, 15143–15146; (*b*) F. Plasser, H. Pašalić, M. H. Gerzabek, F. Libisch, R. Reiter, J. Burgdörfer, T. Müller, R. Shepard and H. Lischka, *Angew. Chem., Int. Ed.*, 2013, **52**, 2581–2584; (*c*) L. Zöphel, R. Berger, P. Gao, V. Enkelmann, M. Baumgarten, M. Wagner and K. Müllen, *Chem.–Eur. J.*, 2013, **19**, 17821–17826.

15 (*a*) J. G. Laquindanum, H. E. Katz and A. J. Lovinger, *J. Am. Chem. Soc.*, 1998, **120**, 664–672; (*b*) Q. Miao, X. Chi, S. Xiao, R. Zeis, M. Lefenfeld, T. Siegrist, M. L. Steigerwald and C. Nuckolls, *J. Am. Chem. Soc.*, 2006, **128**(4), 1340–1345; (*c*) P. Natarajan and M. Schmittel, *J. Org. Chem.*, 2013, **78**, 10383–10394; (*d*) C. F. H. Allen and A. Bell, *J. Am. Chem. Soc.*, 1942, **64**, 1253–1260; (*e*) K. Tanaka, N. Aratani, D. Kuzuhara, S. Sakamoto, T. Okujima, N. Ono, H. Uno and H. Yamada, *RSC Adv.*, 2013, **3**, 15310–15315; (*f*) Z. Sun, Q. Ye, C. Chi and J. Wu, *Chem. Soc. Rev.*, 2012, **41**, 7857–7889.

16 (*a*) S. Toyota, R. Miyaji, Y. Yamamoto, M. Inoue, K. Wakamatsu and T. Iwanaga, *Eur. J. Org. Chem.*, 2015, 7648–7651; (*b*) I. Agranat and Y. Tapuhi, *J. Org. Chem.*, 1979, **44**, 1941–1948.

17 (*a*) *The Aromatic Sextet*, ed. E. Clar, John Wiley & Sons, London, 1972, pp. 81–82; (*b*) E. Clar, *Polycyclic Hydrocarbons, I*, Academic Press, New York, 1964, p. 46.

18 (*a*) J. E. Anthony, D. L. Eaton and S. R. Parkin, *Org. Lett.*, 2002, **4**, 15–18; (*b*) M. L. Tang, A. D. Reichardt, T. Siegrist, S. C. B. Mannsfeld and Z. Bao, *Chem. Mater.*, 2008, **20**, 4669–4676.

19 X. Zhang, J. Li, H. Qu, C. Chi and J. Wu, *Org. Lett.*, 2010, **12**, 3946–3949.

20 (*a*) K. Yamaguchi, *Chem. Phys. Lett.*, 1975, **33**, 330–335; (*b*) K. Yamaguchi, T. Kawakami, Y. Takano, Y. Kitagawa, Y. Yamashita and H. Fujita, *Int. J. Quantum Chem.*, 2002, **90**, 370–385.

21 M. Mamada, H. Katagiri, T. Sakanoue and S. Tokito, *Cryst. Growth Des.*, 2015, **15**, 442–448.

22 T. Wombacher, S. Foro and J. J. Schneider, *Eur. J. Org. Chem.*, 2016, 569–578.

23 (*a*) J. J. Dressler, M. Teraoka, G. L. Espejo, R. Kishi, S. Takamuku, C. J. Gómez-García, L. N. Zakharov, M. Nakano, J. Casado and M. M. Haley, *Nat. Chem.*, 2018, **10**, 1134–1140; (*b*) Y.-C. Hsieh, C.-F. Wu, Y.-T. Chen, C.-T. Fang, C.-S. Wang, C.-H. Li, L.-Y. Chen, M.-J. Cheng, C.-C. Chueh, P.-T. Chou and Y.-T. Wu, *J. Am. Chem. Soc.*, 2018, **140**, 14357–14366.

24 T. Jousselin-Oba, M. Mamada, A. Okazawa, J. Marrot, T. Ishida, C. Adachi, A. Yassar and M. Frigoli, *Chem. Sci.*, 2020, DOI: 10.1039/D0SC04583G.

25 (*a*) G. E. Rudebusch, J. L. Zafra, K. Jorner, K. Fukuda, J. L. Marshall, I. Arrechea-Marcos, G. L. Espejo, R. Ponce Ortiz, C. J. Gómez-García, L. N. Zakharov, M. Nakano, H. Ottosson, J. Casado and M. M. Haley, *Nat. Chem.*, 2016, **8**, 753–759; (*b*) Y.-C. Hsieh, C.-F. Wu, Y.-T. Chen, C.-T. Fang, C.-S. Wang, C.-H. Li, L.-Y. Chen, M.-J. Cheng, C.-C. Chueh, P.-T. Chou and Y.-T. Wu, *J. Am. Chem. Soc.*, 2018, **140**, 14357–14366; (*c*) A. M. Zeidell, L. Jennings, C. K. Frederickson, Q. Ai, J. J. Dressler, L. N. Zakharov, C. Risko, M. M. Haley and O. D. Jurchescu, *Chem. Mater.*, 2019, **31**, 6962–6970; (*d*) T. Jousselin-Oba, M. Mamada, J. Marrot, A. Maignan, C. Adachi, A. Yassar and M. Frigoli, *J. Am. Chem. Soc.*, 2019, **141**(23), 9373–9381.

26 J. G. Champlain, *Appl. Phys. Lett.*, 2011, **99**, 123502.